



Published in final edited form as:

Proteins. 2015 August ; 83(8): 1414–1426. doi:10.1002/prot.24824.

## Molecular modeling of the binding modes of the Iron-sulfur protein to the Jac1 co-chaperone from *Saccharomyces cerevisiae* by all-atom and coarse-grained approaches

Magdalena A. Mozolewska<sup>1,2</sup>, Paweł Krupa<sup>1,2</sup>, Harold A. Scheraga<sup>2</sup>, and Adam Liwo<sup>1,\*</sup>

<sup>1</sup>Faculty of Chemistry, University of Gdansk, ul. Wita Stwosza 63, 80-308 Gdansk, Poland <sup>2</sup>Baker Laboratory of Chemistry and Chemical Biology, Cornell University, Ithaca, NY 14853-1301, USA

### Abstract

The Iron sulfur protein 1 (Isu1) from yeast, and the J-type co-chaperone Jac1, are part of a huge ATP-dependent system, and both interact with Hsp70 chaperones. Interaction of Isu1 and Jac1 is a part of the iron-sulfur cluster biogenesis system in mitochondria. In this study, the structure and dynamics of the yeast Isu1-Jac1 complex has been modeled. First, the complete structure of Isu1 was obtained by homology modeling using the I-TASSER server and YASARA software and thereafter tested for stability in the all-atom force field AMBER. Then, the known experimental structure of Jac1 was adopted to obtain initial models of the Isu1-Jac1 complex by using the ZDOCK server for global and local docking and the AutoDock software for local docking. Three most probable models were subsequently subjected to the coarse-grained molecular dynamics simulations with the UNRES force field to obtain the final structures of the complex. In the most probable model, Isu1 binds to the left face of the “T” shaped Jac1 molecule by the  $\beta$ -sheet section of Isu1. Residues L<sub>105</sub>, L<sub>109</sub>, and Y<sub>163</sub> of Jac1 have been assessed by mutation studies to be essential for binding (Ciesielski et al., *J. Mol. Biol.* 2012, **417**, 1–12). These residues were also found, by UNRES/MD simulations, to be involved in strong interactions between Isu1 and Jac1 in the complex. Moreover, N<sub>95</sub>, T<sub>98</sub>, P<sub>102</sub>, H<sub>112</sub>, V<sub>159</sub>, L<sub>167</sub> and A<sub>170</sub> of Jac1, not yet tested experimentally, were also found important in binding.

Corresponding author: Adam Liwo, Faculty of Chemistry, University of Gdansk, ul. Wita Stwosza 63, 80-308 Gdansk, Poland, phone: +48 58 523 5124, fax: +48 58 523 5472, adam@sun1.chem.univ.gda.pl.

Supporting Information: Figure S1 presents a crystal structure of Jac1 with a marked His-Pro-Asp motif. Figure S2 has a schematic representation of the Fe-S cluster biogenesis cycle based on current state of knowledge. Figure S3 has the results from homology modeling: a) model 4 from I-TASSER; b) model 1 from I-TASSER; c) model 2 from I-TASSER; d) model 3 from I-TASSER; e) hybrid model from YASARA with the respective secondary-structure annotations (H for helix, B for  $\beta$ -strand). The chains are colored from red to blue from the C- to the N-terminus. Figure S4 has the secondary structure of Isu1 predicted by PSI-PRED and alignments of Isu1 sequence to sequences of 10 best templates used in homology modeling. Figure S5 has the Isu1 model quality per residue (score calculated by WHAT\_CHECK based on 16 different quality estimates). Above the line, the diagram shows the region with good prediction. Below the line, the diagram shows the region with worse prediction. Figure S6 is a plot of the RMSD for Isu1 during an all-atom simulation with the YASARA hybrid model using the AMBER force field. Figure S7 is a diagram of number of structures in clusters after initial clustering by AutoDock program. Table S1 illustrates the top 10 structural analogs used by I-TASSER. Table S2 illustrates 10 structurally most similar proteins from the PDB data base used to obtain the models from I-TASSER. Table S3 illustrates the top 3 templates for homology modeling by YASARA. Table S4 provides the number of structures after docking procedure. Table S5 presents results from clustering for Models 1-3 of Isu1-Jac1 complex split into seven groups named A-G. Table S6 illustrates the interactions between Isu1 and three residues from Jac1 (L<sub>105</sub>, L<sub>109</sub>, Y<sub>163</sub>) for model 1 during the simulation. Table S7 illustrates the interactions between Isu1 and three residues from Jac1 (L<sub>105</sub>, L<sub>109</sub>, Y<sub>163</sub>) for model 2 during the simulation. Table S8 illustrates the interactions between Isu1 and three residues from Jac1 (L<sub>105</sub>, L<sub>109</sub>, Y<sub>163</sub>) for Model 3 during the simulation. Section “UNRES force field” includes the expression for the UNRES energy function and the explanation of its terms.

## Keywords

iron-sulfur cluster biogenesis; iron-sulfur protein 1; J-protein; Isu1-Jac1 interactions; UNited RESidue (UNRES) force field; homology modeling

## Introduction

The iron-sulfur (Fe-S) clusters (ISCs) occur in every living organism. They are among the oldest known catalyst cofactors. Fe-S clusters are involved in many activities, which are essential for cell functioning, e.g., as redox reactions, electron transfer, and catalysis of chemical reactions; they also stabilize the structures of many proteins. The iron-sulfur clusters play a crucial role in *Saccharomyces cerevisiae* and in bacterial systems. The release of an Fe-S cluster from Isu1, and its transfer and incorporation into recipient apoproteins (Apo) is facilitated by the components of the ISC assembly machinery including the ATP-dependent Hsp70 chaperone Ssq1 and the DnaJ-like co-chaperone Jac1.<sup>1</sup>

Isu1 is a protein which was highly conserved during evolution. It can be found in many bacteria, and Isu1 equivalents can be found in all eukaryotes. The protein consists of 165 amino-acid residues, of which the first 27 residues are from the mitochondrion sequence. The structure of Isu1 has not yet been determined; however, the structure of its bacterial equivalent, IscU, has been solved by X-ray crystallography.<sup>2</sup> Isu1 contains one iron-sulfur cluster (2Fe-2S) bonded with three cysteine residues, conserved among evolution in different organisms.

The structure of the Isu1 partner, Jac1, has already been determined by X-ray crystallography<sup>3</sup> (pdb: 3UO3) (Figure S1 of the Supporting Information). Jac1 contains 181 amino-acid residues, which form  $\alpha$ -helices arranged in a  $\Gamma$  shape. Like every J-protein, Jac1 contains a J-domain consisting of 74 residues (residues 11-84), in which the His-Pro-Asp motif responsible for binding to Hsp70 is highly conserved, and C-terminal C-domain (residues 101-184) connected to the J-domain by a flexible linker (residues 85-100).<sup>3</sup> The main function of Jac1 is to stimulate the ATPase activity of Hsp70, and move the Isu1 to Hsp70 – Ssq1.<sup>3</sup>

Experimental studies suggest that Jac1 interacts with Isu1 mainly through residues L<sub>105</sub>, L<sub>109</sub>, and Y<sub>163</sub><sup>3</sup>; However, it was reported that residues L<sub>104</sub>, K<sub>107</sub>, D<sub>110</sub>, D<sub>113</sub>, E<sub>114</sub>, and Q<sub>117</sub> are also involved.<sup>4</sup> Isu1 interacts with Ssq1 and Jac1 through two separate binding sites, one comprised of the LPPVK motif<sup>5, 6</sup> and another one consisting of residues L<sub>63</sub>, V<sub>72</sub>, and F<sub>94</sub>, respectively.<sup>7</sup>

Although the mechanism of iron-sulfur cluster biogenesis has not yet been discovered, it is clear that the formation of a complex between Isu1 and Jac1 is a crucial step in the transfer of the Fe-S cluster to the target proteins (Figure S2 and section “Fe-S cluster cycle” of Supporting Information). However, despite the effort of many researchers,<sup>3, 8, 9, 10, 11, 12, 13, 14</sup> the structure of the complex and interactions that contribute to its formations have not been fully determined.

The aim of this work was to model the structure and stability of the Isu1-Jac1 complex, which is a crucial one in the entire process of Fe-S cluster biogenesis in yeast. An initial attempt at modeling the binding mode of Isu1 to Jac1 was made recently by using a combination of template-based modeling and molecular docking.<sup>15</sup> However, those studies were based on an incomplete Isu1 model (without the N-terminal H1 helix) and only limited rigid docking with the ZDOCK was carried out without assessment of the stability of the proposed complex.

Because no experimental structure of Isu1 is available, we used homology modeling to obtain the initial structure of this protein which, after stability tests and refinement, was used to create the possible structures of the complex with Jac1 by using ZDOCK server and AutoDock software. To assess the stability of the resulting complexes, molecular dynamics simulations with the coarse-grained UNited RESidue (UNRES) force field (Figure 1) developed in our laboratory<sup>16</sup> were carried out. The simplification of the representation of polypeptide chains in the UNRES model enabled us to extend the time scale of simulations by 4 orders of magnitude compared to that of all-atom simulations.<sup>17, 18</sup> We have already used the UNRES force field to investigate the transition from the closed (ADP-bound) to the open (ATP-bound) conformation of the DnaK Hsp70 chaperone from *E. coli*.<sup>19</sup> The structure of the open conformation was determined by X-ray crystallography<sup>20</sup> after our work was published and was very close to that predicted by UNRES/MD. UNRES has also been featured in the last Community-Wide Experiment of the Assessment of Techniques for Protein Structure Prediction (CASP10), because it was one of the only two methods that found the correct domain packing of target T0663,<sup>21</sup> which is remarkable because T0663 seemed to be a comparative-modeling and not a free-modeling target. Knowledge-based methods predicted the structure of each of the two domains of T0663 with a very good accuracy but none of them found correct packing of domains. Thus, UNRES appears to be an appropriate tool to study the phenomena that involve multi-domain proteins, such as binding of molecular chaperones.

## Materials and Methods

### Modeling the Isu1 structure

The sequence of Isu1 consists of two parts; residues 1-27 correspond to the transit peptide, which is the fragment responsible for directing the protein to the mitochondrion, while residues 28-165 constitute the main protein chain. Mature proteins that perform functions in organelles (e.g. mitochondria) usually do not have the signal peptide.<sup>22,23,24</sup> Therefore, in the present work only the 28-165 part of the sequence was used in homology modeling.

We used the Iterative Threading ASSEmbly Refinement (I-TASSER) server<sup>25</sup> and the YASARA (Yet Another Scientific Artificial Reality Application)<sup>26</sup> software to model the unknown structure of Isu1.

The best model was subjected to refinement (relaxation) by all-atom molecular dynamics with the AMBER11 package<sup>27</sup>. In the first step, the energy was minimized by the steepest-descent and conjugate-gradient algorithms. Combining these two algorithms provides the best results because the steepest-descent algorithm is more efficient and stable when far

from the minimum (therefore, it brings the system to the neighborhood of the minimum quickly), while the conjugated-gradient is much more efficient in close proximity to the minimum.<sup>28,29</sup> Subsequently, an all-atom MD simulation was performed with the AMBER FF99SB force field<sup>30</sup> and the TIP3P water model.<sup>31</sup> A 9 Å cut-off was imposed on the nonbonded interactions described by the Lennard-Jones potential, while particle-mesh Ewald summation was used to compute electrostatic interactions.<sup>32</sup> The simulations were run in a periodic box with TIP3P water under isothermal–isobaric (NTP) conditions at T = 300 K and p = 1 atm. A simulation was run for 100 ns with a 2 fs time step; coordinates and energy were saved every 1000 steps.

### Determining the binding modes of Isu1 to Jac1

To determine the probable binding modes of Isu1 and Jac1, we used ZDOCK<sup>33</sup> and AutoDock 4.2.3.<sup>34</sup> As initial structures, the Isu1 structure obtained by homology modeling and subsequent MD refinement (see section Modeling the Isu1 structure) and the crystallographic structure<sup>3</sup> of Jac1 (PDB code 3UO3) were used. ZDOCK performed a global grid search in position and orientation of Jac1 with respect to Isu1, with local docking (more detailed docking in the space restricted to the C-terminal domain of Jac1) to explore the neighborhood of Jac1 with the lowest energy in more detail.<sup>33</sup> The ZDOCK server is set to produce 2000 structures of complexes in global docking and a smaller subset in restricted docking.

After the extensive search of the docking space with ZDOCK was accomplished, more detailed exploration (local docking) was performed by AutoDock<sup>34</sup> 4.2.3, which uses a grid search and a genetic algorithm to find the binding mode. The original code of AutoDock 4.2.3 is applicable to dock only small ligands to proteins and we, therefore, modified it to extend it to protein-protein docking by increasing the maximum allowed ligand size and maximum number of grid points in each dimension (from 128 to 256) to maintain accuracy. The modified AutoDock program was set to generate 500 binding-site predictions. Modified versions of the AutoDock program have been successfully used in protein-protein docking in the past.<sup>35</sup> Combining the coarse-grid search of the docking space with ZDOCK with finer local search with AUTODOCK (which, however, has been originally designed for docking small ligands) and with subsequent coarse-grained molecular dynamics is likely to result in finding all reasonable structures of the Isu1/Jac1 complex.

### All-atom MD simulations with AMBER force field

After obtaining the initial structures of the Isu1-Jac1 complex, we performed molecular-dynamics simulations with the AMBER force field. The number of water molecules was between 19632 (for Model 3) and 22625 (for Model 1). Each simulation was run for 100 ns with a time step of 2 fs. Snapshots were saved every 1000 steps. The dimensions of the periodic boxes varied from about 63 Å × 89 Å × 115 Å for Model 3 to 105 Å × 106 Å × 66 Å for Model 1.

## Coarse-grained MD simulations with UNRES

We used the speed-up advantage of the UNRES (UNited RESidue) coarse-grained physics-based force field developed in our laboratory to perform extensive MD simulations of the Isu1-Jac1 complex in a much larger time-scale than using all-atom force fields.

In the UNRES model,<sup>16, 36, 37, 38</sup> a polypeptide chain is represented by a sequence of united peptide groups (p), each of which is placed between the two consecutive C $\alpha$  atoms, and united side chains (SC) (represented by ellipsoids of revolution) attached to the C $\alpha$  atoms. Only the SC and p centers are interaction sites; the  $\alpha$ -carbon atoms serve only to define the geometry of a chain (Figure 1).

The UNRES force field originates from the potential of mean force of a protein in aqueous environment, which has been expanded into a cluster-cumulant series to give an implementable energy function. This energy function is given by equation 2 of the Supporting Information.

Canonical coarse-grained MD simulations were run with the Langevin scheme and the VTS (variable time step) algorithm<sup>16, 17</sup> at temperature  $T = 300$  K. To speed up the calculations, the viscosity of water was scaled down by a factor of 0.01 as in our earlier work<sup>16, 17</sup>. Sixteen independent trajectories were run for each simulation. Each trajectory consisted of 40 million steps of 4.89 fs length; this makes about 200 ns of total UNRES time. However, because of time-scale distortion, resulting from averaging over the secondary degrees of freedom and scaling down the water friction coefficient<sup>17</sup>, the length of a simulation corresponds to at least 200  $\mu$ s of real time. Each of the 16 trajectories was started from structures of one of three models.

## Clustering

Cluster analysis was performed by using Ward's Minimum Variance Method.<sup>39, 40, 41</sup> This method provides the most balanced partitioning of the set of conformations.<sup>41</sup> For each simulation, all 16 trajectories were analyzed simultaneously. The C $\alpha$ RMSD was chosen as a measure of the distance between the groups of conformations, and the cut-off value was 14 Å. With this cut-off value, the number of groups is reasonably low, while the structures that belong to one group are still similar. The relatively high value of the cut-off results from use of the minimum-variance method in which the cut-off is related to the distance between the centers of the clusters and not to that of the closest elements of two different clusters. Moreover, because a molecular complex is analyzed, even a small displacement of its components can result in a significant RMSD.

## Mutations of Isu1 and Jac1 in the complex

To verify the importance of selected interactions between amino-acid residues in the obtained most probable model of the Isu1-Jac1 complexes (Model 3), selected residues of Jac1 were replaced with alanine residues and the stability of the resulting complexes was assessed by MD simulations with the UNRES force field. The mutated residues were L<sub>105</sub>, L<sub>109</sub> and Y<sub>163</sub> for the first mutant, L<sub>105</sub> and L<sub>109</sub> for the second mutant, and Y<sub>163</sub> for the third mutant, respectively. In the fourth mutation, the residues involved in the formation of a

salt bridges between Isu1 and Jac1 (D<sub>18</sub>, K<sub>20</sub>, G<sub>41</sub>, R<sub>39</sub> of Isu1 and D<sub>113</sub>, Q<sub>117</sub>, D<sub>119</sub>, K<sub>178</sub> of Jac1) were changed to alanine; finally, L<sub>105</sub>, L<sub>109</sub> and Y<sub>163</sub> of Jac1 and the residues involved in salt bridges were mutated to give Isu1<sub>DKGR</sub>Jac1<sub>DQDK</sub>. Each mutated complex was subjected to coarse-grained MD simulations using the variant of the UNRES force field parameterized with the 1GAB protein<sup>16</sup>. The conditions of the simulations are those described in section “Coarse-grained MD simulations with UNRES”

## Results and Discussions

### Modeling the Isu1 structure

Isu1 was modeled in a previous study;<sup>15</sup> however, only part of the sequence of this protein had been considered<sup>15</sup> and the model was not optimized and validated by molecular dynamics simulations. We, therefore, decided to model the structure of this protein for the purpose of our study, by using the state-of-the-art molecular modeling tools available.

The best ten templates used for modeling by the I-TASSER server were from four different organisms: *Mus musculus*, *Escherichia coli*, *Haemophilus influenzae*, and *Aquifex aeolicus*. Each of these templates is an IscU protein and is functionally related to Isu1. For almost every template, the percentage of sequence identity in the threading-aligned region with that of the query sequence was above 0.66. The sequence identity of the whole template chains with the query sequence was also above 0.66. The normalized Z-score of the threading alignments was above 2.7 for all templates, which means that the prediction is very good (Table S1).

The following three proteins 3LVL, 1WFZ, 2Z7E, which are analogs of the Isu1 – IscU proteins from different organisms, were used as the main templates to predict a structure of Isu1 by YASARA. The sequence similarity of the templates to Isu1 is above 96% in all three, which shows that the model built on the basis of these proteins is probably a very good one (Table S3). The ‘hybrid’ model was created based on the highest-score template (with a YASARA score of 191.13 in Table S3); however, information of structures of two template proteins mentioned above with the highest homology to the target sequence was also utilized.

The best model of Isu1 was selected based on the Z-score value (Table 1) and on the quality of secondary structure (Figure S4) of the predicted fragments of the protein. More details about the models are available in section “Modeling the Isu1 structure” of the Supporting Information.

### Isu1-Jac1 docking

Using the predicted structure of Isu1, we carried out global docking of Isu1 to Jac1, for which we used the crystallographic structure of Jac1 with PDB code: 3UO3. ZDOCK<sup>33</sup> was implemented to identify the regions in Jac1 where Isu1 can potentially bind. Three main docking positions were identified (Figure 2), by clustering 100 complexes, from a total of 2000, based on the highest values of the ZDOCK score<sup>42</sup> function, of which only one (part C shown in Figure 2), in which Isu1 makes contact with helices H4, H5 and H7 of Jac1, is consistent with the experimental data.<sup>3</sup>



After the approximate docking position was found by global docking, the docking space was explored in more detail (by local docking), using ZDOCK and modified AutoDock. As a result, a set of 196 structures from restricted docking by using ZDOCK and a set of 500 structures from AutoDock were obtained. Structures from AutoDock were clustered based on RMSD and binding energy criteria with default cut-offs, 2Å and 0.5 kcal/mol, respectively, obtaining nine clusters with populations higher than 2% of the total population (more than 10 structures) (Figure S7 in Supporting Information). It has to be noted, that the binding energy calculated by AutoDock is distorted, because of the simplifications that we made to handle such a large ligand. On that basis, we grouped nine representative structures from AutoDock and ten structures from ZDOCK restricted docking with the highest values of the ZDOCK score function into three main clusters (Figure 3). In the first model (Model 1) of the Isu1-Jac1 complex (Figure 3A), Isu1 binds mainly to the H2 helix of Jac1. In the second model (Model 2, Figure 3B), Isu1 binds mainly to the H5 helix of Jac1. In the third model (Model 3, Figure 3C), the B1, B2, B3 strands of Isu1 bind to Jac1. Model 3 (Figure 3C) appeared to be the most probable (Table S4), because the interactions between residues of the B1, B2, B3  $\beta$ -strands of Isu1 and those of the H4, H5 and H7 helices in Jac1 were found experimentally.<sup>3</sup> Model 3 is also similar to a preliminary model obtained for the Isu1/Jac1 complex found in a previous study<sup>15</sup> by homology modeling and docking. However, it should be noted that that model was not subjected to optimization or stability tests.<sup>15</sup> Our studies also suggest that this is the most probable model, because this type of docking was the most common in the complexes obtained by local docking (Table S4). However, we did not have enough evidence to discard two other models (Figure 3B and Figure 3C); at this stage, therefore, all three models were used for further investigation.

### MD simulations of the Isu1-Jac1 complex

To analyze the resulting models of the Isu1-Jac1 complex, we initially tried to use all-atom MD, which is a popular method for relaxing and refining the structures of the protein-protein complexes obtained by crude molecular docking,<sup>43</sup> and for the analysis of the dynamics of the system. Given the available computer resources, we could run only about 100 ns MD simulations with the AMBER force field. During this short period of simulation time, we did not observe any major conformational changes in the systems studied but only some local fluctuations. Therefore, to complete the exploration of the docking space, we performed MD simulations with the coarsegrained UNRES force field. Such an approach provides a much more extensive conformational search than the all-atom approach, because using the coarse-grained UNRES force field, enables us to run large-scale simulations.<sup>37</sup> The simulations were started from the structures of the three models of the Isu1-Jac1 complex (Model 1, Model 2 and Model 3) and the mutants of Model 3. Structures from the trajectories obtained in all runs (16 runs) for a given model were joined together to perform a cluster analysis. To simplify the analysis, key structures from all clusters of all models were determined and analyzed for similar orientations of Isu1 with respect to Jac1 to arrange them into groups of similar conformations, as described in the next subsection. Representative structures of each group are shown in Figure 4.

## Analysis of UNRES/MD trajectories of the Isu1-Jac1 complex

The structures of the Isu1-Jac1 complex obtained by local docking followed by UNRES/MD simulations, as described in the previous section, can be split into seven groups (Table S5 in the Supplement) from which two (C and E in Figure 4.) are the largest and the most populated in all models. During the MD simulations, the structures of Isu1 and Jac1 drifted from the initial structures of isolated molecules in order to form favorable interactions in the complex; the respective RMSD values are shown in Table 2. It can be observed, that the predicted structure of Isu1 is very stable and quite rigid (RMSD up to 5.292 Å, which value is of the order of the resolution of the coarse-grained UNRES force field for proteins with this size). The structure of Jac1 is more flexible due its two-domain composition; the RMSD of the whole structure is up to 9.829 Å.

### Model 1

Analysis of the clustering results of the Model 1 trajectories shows that group A dominates (Figure 6). Group A contains 42.6% of all structures in all time sections of the simulations and more than half of the structures at the end of the simulations. This group represents the structures in which Isu1 binds to Jac1 by the upper side of Isu1 (N-terminus) (Figure 4A). The remaining groups are less populated and the second largest one (group B), which contains 20.1% of all structures, is very similar in structure to group A. The interactions between Isu1 and Jac1 in group B involve the upper side and part of the  $\beta$ -sheets of Isu1 (Figure 4B). Even less populated is group D (13.8% of all structures), in which part of the  $\beta$ -sheets of Isu1 bind to helix H5 of Jac1 (Figure 4D). It is worth noting that, in this group, Isu1 is rotated by 180° with respect to Jac1, an orientation different from that in all other groups. The binding patterns of Isu1 to Jac1 are visualized in the contact maps shown in Figure 5.

A detailed analysis of the interactions in Model 1, 2 and 3 is presented in the Supporting Information.

### Model 2

For Model 2 of the Isu1-Jac1 complex (Figure 6), it can be observed that groups C and E together comprise the majority of structures (60.6% and 21.2% of all structures, respectively). Group C contains the structures in which, helix H5 of Isu1 and part of the  $\beta$ -sheets of Isu1 bind to Jac1, while group E (Figure 4E) represents the structures for which the  $\beta$ -strands of Isu1 are connected to Jac1; these structures are very similar to Model 3 obtained by docking (Figure 3C).

### Model 3

Two main binding modes can be observed in MD simulations started from Model 3. These binding modes are represented by the largest groups E (42.6% of all structures) and G (33.8% of all structures) respectively of Figure 6. Group E comprises the structures of the complex in which the  $\beta$ -sheet part of Isu1 binds to Jac1, as in the starting structure (Figure 3C) but a little lower (below helix H5 from Jac1). Group G represents the structures in which Isu1 binds to Jac1 by the upper side (especially with helix H1 from Isu1) and part of the  $\beta$ -sheets of Isu1.



### Summary of MD simulations of Models 1, 2 and 3

Simulations started from Models 1, 2 and 3 often have resulted in conformations in which Isu1 binds to Jac1 through the  $\beta$ -sheets and upper part of Isu1. These structures are represented by group 6E and also are similar to those of group 6C (in which Isu1 and Jac1 also interact through the H5 helix of Isu1), 6D (they differ in the rotation of Isu1), and 6A (some interactions through  $\beta$ -sheets, mostly involving the upper part of Isu1) (Figure 5). In Figure 6 the numbers of structures in each group, obtained by starting from the three models, are presented. Groups C and E are the most populated. The third most populated group is group A, whose high population may be caused by lack of Fe-S clusters in our simulations. If the Fe-S cluster were present, Isu1 probably would not be able to slide that much to interact only by the upper-side.

We also observed strange structures of Isu1-Jac1 in trajectories started from Models 2 and 3, in which the structure of Jac1 partially unfolded to form a globular complex with Isu1 (Figure 4F). In this structure, the whole interaction interface is different from that in other groups (Figure 5).

The residues which were found by the experiments<sup>3</sup> to be important in binding Isu1 to Jac1 are found to be involved in binding in the simulations. They appear mostly in groups C and E, which are similar to Model 3 generated by global and local docking. Therefore, Model 3 seems to be the most probable model of the Isu1-Jac1 complex. In addition to this, other residues whose roles in binding were not yet explored experimentally, were predicted by our simulations to be involved in binding (Figure 5). To confirm this, we performed UNRES/MD simulations for several variants of the complex in which residues that were found involved in binding were replaced with the alanine residues.

### Assessment of the importance of interactions by mutational analysis

The initial structures of the mutants for the UNRES/MD simulations were obtained from the structure of Model 3 from the local docking by replacing one or more residue with alanine. The following variants of Jac1 were created: Y<sub>163</sub>→A (hereafter referred to as Jac1<sub>Y</sub>), L<sub>105</sub>→A, L<sub>109</sub>→A (hereafter referred to as Jac1<sub>LL</sub>), L<sub>105</sub>→A, L<sub>109</sub>→A, Y<sub>163</sub>→A (hereafter referred to as Jac1<sub>LLY</sub>), and D<sub>113</sub>→A, Q<sub>117</sub>→A, D<sub>119</sub>→A, K<sub>178</sub>→A in Jac1 and D<sub>18</sub>→A, K<sub>20</sub>→A, G<sub>41</sub>→A, R<sub>39</sub>→A in Isu1 (hereafter referred to as Jac1<sub>DQDK</sub>Isu1<sub>DKGR</sub>). For each mutation, the trajectories were joined together and cluster analysis was performed to determine the key structures that occurred during the simulations. After clustering, several groups of structures were obtained for each mutation, which we used to simplify further analysis.

Detailed analysis of the influence of each mutation on the structure of the Isu1-Jac1 complex is described in section “Interaction analysis in Models 1, 2, and 3” of the Supporting information.

The results of mutational analysis confirm that the L<sub>105</sub>, L<sub>109</sub>, and Y<sub>163</sub> residues of Jac1 are important for the binding of Isu1 to Jac1. Not every mutation has a direct influence on binding Isu1; the Jac1<sub>Y</sub> mutation influences Jac1 structure, which facilitates the change of the binding mode (Figure 7). The general behavior of the Isu1-Jac1 system is that the most

stable structures are those of group E (Figure 4E), which are similar to Model 3 (Figure 4C) but, without mutations, the structure similar to Model 2 (group C; Figure 4C) is also observed in some simulations. The Jac1<sub>LL</sub> and Jac1<sub>DQDK</sub>Isu1<sub>DKGR</sub> mutations usually change the structure; Isu1 interacts with Jac1 mostly by the upper side of Isu1 which sometimes enters the space between helices H5 and H7 of Jac1 (group H; Figure 4H). MD simulations show that mutations that involve the replacement of two leucines in Jac1, in most cases, converge to group B structures, while the mutations in which tyrosine is replaced with alanine usually result in structures of E (similar to the starting structure) and group A, in which Isu1 interacts only by its upper side with Jac1 (Figure 8).

It can also be observed that, especially for the Jac1<sub>LL</sub> mutation, an unusual amount of structures appears in which Isu1 binds to Jac1 in the upside-down position compared to every other structures of the complex, that interact with Jac1 mostly by the upper side of the  $\beta$ -sheets of Isu1 (group B and H; Figure 4H). This observation suggests that the Jac1<sub>LL</sub> mutation can disrupt the standard contacts between the two proteins. It is also surprising that this effect is much smaller for the Jac1<sub>LLY</sub> mutation.

### Analysis of the binding interface of the Isu1-Jac1 complex

An analysis of the residues of Isu1 and Jac1 involved in the interactions between these two proteins based on UNRES/MD simulations started from three different orientations of wild type proteins (Models 1-3), and with mutations on Jac1 described earlier in the text reveal, that, in each group of structures, there are the same pairs of interacting residues (Figure 5). Averaging the contact maps for groups A-H showed that the deepest minima of residue-residue distance occur for the residues that were found important, based on mutation experiments, for the functioning of yeast cells (and, thereby, should be essential for binding Jac1 to Isu1);<sup>3, 15</sup> these are residues L<sub>105</sub>, L<sub>109</sub>, and Y<sub>163</sub> of Jac1, which are located on the H5, H6, and H8 helices of Jac1, and residues L<sub>63</sub>, and V<sub>72</sub>, and F<sub>94</sub> of Isu1, which are located on the B1, B2, and B3 strands of Isu1, respectively. Residues L<sub>104</sub>, K<sub>107</sub>, D<sub>110</sub>, D<sub>113</sub>, E<sub>114</sub>, and Q<sub>117</sub> of Jac1, which were also suggested to be involved in binding based on mutation experiments, also form contacts with the residues of Isu1 located at the binding interface (Figure 5). Moreover, our study predicts that residues N<sub>95</sub>, T<sub>98</sub>, P<sub>102</sub>, H<sub>112</sub>, located on the B1-B3 strands of Isu1, and V<sub>159</sub>, L<sub>167</sub>, A<sub>170</sub> and W<sub>174</sub>, located on the H5 helix of Isu1, and, to a lesser extent, E<sub>91</sub>, V<sub>108</sub>, S<sub>116</sub>, and E<sub>160</sub> of Isu1 also contribute to binding (Figure 5). The possible involvement of helix H5 of Isu1 in binding is new with respect to the experimental work on the Jac1/Isu1 binding. The interface on Jac1 predicted by our study, in addition to the residues found experimentally important for binding, also comprises V<sub>64</sub>, A<sub>66</sub>, D<sub>71</sub>, M<sub>73</sub>, R<sub>74</sub>, K<sub>92</sub>, T<sub>93</sub>, C<sub>96</sub> and, to a lesser extent, G<sub>65</sub>, G<sub>70</sub>, G<sub>95</sub>, V<sub>135</sub>, Lys<sub>136</sub>, H<sub>138</sub>, C<sub>139</sub>, and L<sub>142</sub>. The binding interface is visualized in Figure 9. This observation extends the conclusions drawn from experimental studies regarding the structure of the complex and explains why the complex is stable even if the residues that could form intermolecular salt bridges are replaced with alanines.

## Conclusions

In this work, a reliable model of the complete structure of the Isu1 protein was constructed by using homology modeling methods and tested for stability by MD simulations with the all-atom AMBER<sup>27</sup> force field. The resulting Isu1 structure was subsequently docked to Jac1 by using the ZDOCK<sup>33</sup> and AutoDock<sup>34</sup> software. The resulting structures were grouped in 3 clusters, termed Models 1-3 (Figure 3), and were subsequently used as initial structures for MD simulations with the UNRES force field<sup>16, 38, 44</sup>. This flexible docking by UNRES/MD was necessary because the initial structures obtained by rigid docking could contain unfavorable interactions (clashes) that could be eliminated upon small deformation of the components (i.e., induced fitting). These calculations were only possible with use of a coarse-grained representation of the system, which accelerates the computation time by more than 3 orders of magnitude<sup>17</sup>. To assess which interactions are important for the stability of the Isu1-Jac1 complex, UNRES/MD simulations were also carried out for the variants of the complex in which selected residues were replaced with alanines. As a result, 8 groups (A-H) of structures of the Isu1-Jac1 complex with different orientation of the two proteins with respect to each other were obtained, of which groups C and E are the most abundant (Figure 6).

In the structures corresponding to the most populated groups C and E, the  $\beta$ -sheet section and, partially, helix H5 of Isu1 are docked to helices of the outer side of the C-terminal domain of Jac1 (Figure 4C and 4E). This binding mode is in full agreement with the experimental findings that residues L<sub>105</sub>, L<sub>109</sub>, and Y<sub>163</sub> of Jac1 and residues L<sub>63</sub>, and V<sub>72</sub>, F<sub>94</sub> of Isu1<sup>3</sup> are functionally important. Additionally, in the experimental structure of the bacterial equivalent of the Isu1-Nfs1 complex (IscU-IscS) (pdb code: 3LVL)<sup>45</sup> the crucial interface residues are located in the H1 helix and part of the  $\beta$ -sheets of the Isu1 analog. Experimental studies<sup>15</sup> strongly suggest that the binding interface of Isu1 in the Isu1-Jac1 complex is very similar to that of Isu1 in the Isu-Nfs1 complex because Jac1 competes with Nfs1 for a binding site.

In addition to confirming that the residues already found to be important for the Isu1-Jac1 binding by experimental mutagenesis studies, other interactions that could also be essential for the Isu1-Jac1 binding were also predicted by our simulations; these are discussed in detail in section “Analysis of the binding interface of the Isu1-Jac1 complex”. In particular, the simulations suggest that, apart from the B1-B3 strands, helix H5 of Isu1 could be involved in binding. These findings constitute a solid basis for further experimental mutagenesis studies directed at understanding the iron-sulfur cluster transfer.

## Supplementary Material

Refer to Web version on PubMed Central for supplementary material.

## Acknowledgments

We thank Dr. Jarosław Marszałek (Intercollegiate Faculty of Biotechnology, University of Gdańsk and Medical University of Gdańsk, Poland) for helpful comments on the manuscript.

This work was supported by the Foundation for Polish Science (grant MPD/2010/5; project operated within the Foundation for Polish Science International PhD Projects (MPD) Programme co-financed by the EU European Regional Development Fund, Operational Program Innovative Economy 2007-2013), the U.S. National Institutes of Health (grant GM-14312) and the U.S. National Science Foundation (grant MCB10-19767), and conducted by using the resources of (a) our 588-processor Beowulf cluster at the Baker Laboratory of Chemistry and Chemical Biology, Cornell University, (b) the Informatics Center of the Metropolitan Academic Network (IC MAN) in Gdańsk, (c) and our Beowulf cluster at the Faculty of Chemistry, University of Gdańsk.

## References

1. Lill R, Mühlenhoff U. Maturation of iron-sulfur proteins in eukaryotes: mechanisms, connected processes, and diseases. *Annu Rev Biochem.* 2008; 77:670–700.
2. Jeyakanthan, J.; Kanaujia, SP.; Sekar, K.; Agari, Y.; Ebihara, A.; Shinkai, A.; Kuramitsu, S.; Yokoyama, S. Crystal structure of Iron-sulfur cluster biosynthesis protein IscU (TTHA1736) from *thermus thermophilus* HB8. 2007. <http://www.ncbi.nlm.nih.gov/Structure/mmdb/mmdbsrv.cgi?uid=2QQ4>
3. Ciesielski S, Schilke B, Osipiuk J, Bigelow L, Mulligan R, Majewska J, Joachimiak A, Marszalek J, Craig Ea, Dutkiewicz R. Interaction of J-Protein Co-Chaperone Jac1 with Fe-S Scaffold Isu Is Indispensable In Vivo and Conserved in Evolution. *J Mol Biol.* 2012; 417:1–12. [PubMed: 22306468]
4. Andrew AJ, Dutkiewicz R, Knieszner H, Craig E, Marszalek J. Characterization of the interaction between the J-protein Jac1p and the scaffold for Fe-S cluster biogenesis, Isu1p. *J Biol Chem.* 2006; 281(21):14580–14587. [PubMed: 16551614]
5. Dutkiewicz R, Schilke B, Cheng S, Knieszner H, Craig EA, Marszalek J. Sequence-specific interaction between mitochondrial Fe-S scaffold protein Isu and Hsp70 Ssq1 is essential for their in vivo function. *J Biol Chem.* 2004; 279(28):29167–29174. [PubMed: 15123690]
6. Hoff KG, Cupp-Vickery JR, Vickery LE. Contributions of the LPPVK motif of the iron-sulfur template protein IscU to interactions with the Hsc66-Hsc20 chaperone system. *J Biol Chem.* 2003; 278(39):37582–37589. [PubMed: 12871959]
7. Craig EA, Marszalek J. Hsp70 Chaperones. *Encyclopedia of Life Sciences.* 2011
8. Lill R. Iron-sulfur clusters: Basic building blocks for life. *Int J Parasito.* 2007; 1(3):17–20.
9. Lesuisse E, Lyver E, Knight S, Dancis A. Role of YHM1, encoding a mitochondrial carrier protein, in iron distribution of yeast. *Biochem J.* 2004; 378:599–607. [PubMed: 14629196]
10. Alves R, Herrero E, Sorribas A. Predictive reconstruction of the mitochondrial iron–sulfur cluster assembly metabolism: I. The role of the protein pair ferredoxin–ferredoxin reductase (Yah1–Arh1). *Proteins Struct Funct Bioinforma.* 2004; 56:354–366.
11. Marada A, Allu P, Murari A, PullaReddy B, Tammineni P, Thiriveedi V, Danduprolu J, Sepuri N. Mge1, a nucleotide exchange factor of Hsp70, acts as an oxidative sensor to regulate mitochondrial Hsp70 function. *Mol Biol Cell.* 2013; 24:692–703. [PubMed: 23345595]
12. Mühlenhoff U, Gerber J, Richhardt N, Lill R. Components involved in assembly and dislocation of iron–sulfur clusters on the scaffold protein Isu1p. *EMBO J.* 2003; 22:4815–4825. [PubMed: 12970193]
13. Rouhier N, Couturier J, Johnson M, Jacquot J. Glutaredoxins: roles in iron homeostasis. *Trends Biochem Sci.* 2010; 35:43–52. [PubMed: 19811920]
14. Uzarska M, Dutkiewicz R, Freibert S, Lill R, Mühlenhoff U. The mitochondrial Hsp70 chaperone Ssq1 facilitates Fe/S cluster transfer from Isu1 to Grx5 by complex formation. *Mol Biol Cell.* 2013; 12:1830–1841. [PubMed: 23615440]
15. Majewska J, Ciesielski SJ, Schilke B, Kominek J, Blenska A, Delewski W, Song JY, Marszalek J, Craig EA, Dutkiewicz R. Binding of the chaperone Jac1 protein and cysteine desulfurase Nfs1 to the iron-sulfur cluster scaffold Isu protein is mutually exclusive. *J Biol Chem.* 2013; 288(40): 29134–29142. [PubMed: 23946486]
16. Liwo A, Khalili M, Czaplewski C, Kalinowski S, Ołdziej S, Wachucik K, Scheraga H. Modification and optimization of the united-residue (UNRES) potential energy function for canonical simulations. I. Temperature dependence of the effective energy function and tests of the optimization method. *J Phys Chem B.* 2007; 111:260–285. [PubMed: 17201450]

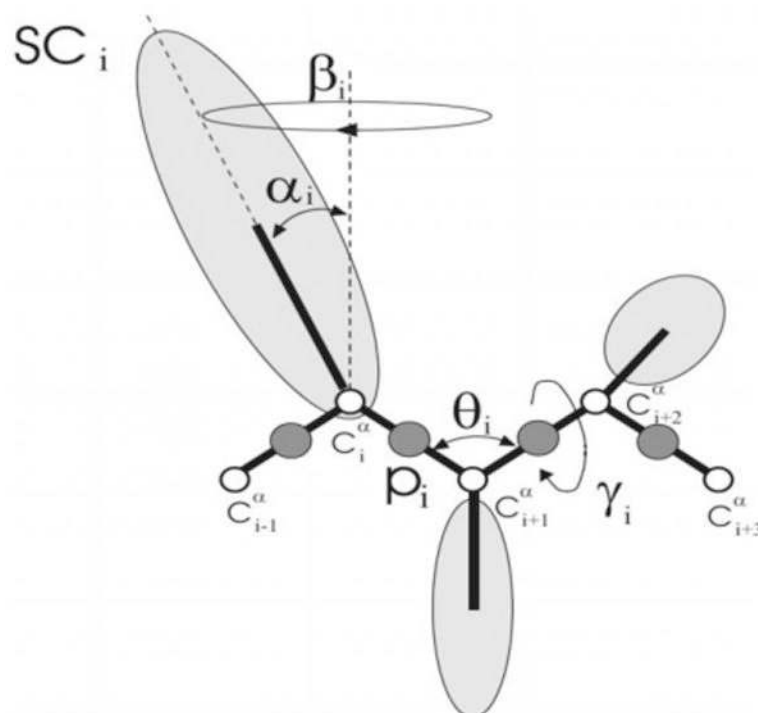
17. Khalili M, Liwo A, Jagielska A, Scheraga H. Molecular dynamics with the united-residue model of polypeptide chains. II. Langevin and Berendsen-bath dynamics and tests on model  $\alpha$ -helical systems. *J Phys Chem B*. 2005; 109(28):13798–13810. [PubMed: 16852728]
18. Liwo A, Khalili M, Scheraga H. Ab initio simulations of protein-folding pathways by molecular dynamics with the united-residue model of polypeptide chains. *Proc Natl Acad Sci U S A*. 2005; 102:2362–2367. [PubMed: 15677316]
19. Goła E, Maisuradze G, Senet P, Oldziej S, Czaplewski C, Scheraga HA, Liwo A. Simulation of the opening and closing of Hsp70 chaperones by coarse-grained molecular dynamics. *J Chem Theory Comput*. 2012; 12:1750–1764. [PubMed: 22737044]
20. Schuermann JP, Jiang J, Cuellar J, Llorca O, Wang L, Gimenez LE, Jin S, Taylor AB, Demeler B, Morano KA, Hart PJ, Valpuesta JM, Lafer EM, Sousa R. Structure of the Hsp110:Hsc70 nucleotide exchange machine. *Mol Cell*. 2008; 31(2):232–243. [PubMed: 18550409]
21. He Y, Mozolewska M, Krupa P, Sieradzan A, Wirecki T, Liwo A, Kachlishvili K, Rackovsky S, Jagieła D, Ślusarz R, Czaplewski C, Oldziej S, Scheraga HA. Lessons from application of the UNRES force field to predictions of structures of CASP10 targets. *Proc Natl Acad Sci U S A*. 2013; 110(37):14936–14941. [PubMed: 23980156]
22. Rosse, AH.; Harrison, JS. *The Yeasts: Yeast Technology*. Elsevier Science; 2012.
23. Rupp, B. *Biomolecular Crystallography: Principles, Practice, and Application to Structural Biology*. Garland Science; 2009.
24. Teixeira PF, Glaser E. Processing peptidases in mitochondria and chloroplasts. *Biochim Biophys Acta*. 2013; 1833(2):360–370. [PubMed: 22495024]
25. Zhang Y. I-TASSER server for protein 3D structure prediction. *BMC Bioinformatics*. 2008; 9(1): 40. [PubMed: 18215316]
26. Venselaar H, Joosten R, Vrolijk B, Baakman C, Hekkelman M, Krieger E, Vriend G. Homology modelling and spectroscopy, a never-ending love story. *Eur Biophys*. 2010; 39(4):551–563.
27. Case D, Cheatham T. The Amber biomolecular simulation programs. *J Comput Chem*. 2005; 26(16):1668–1688. [PubMed: 16200636]
28. Bartholomew-Biggs, MC. The Steepest Descent Method In: *Nonlinear optimization with financial applications*. Springer; 2005. p. 51–64.
29. Shi Z, Guo J. A new family of conjugate gradient methods. *J Comput Appl Math*. 2009; 224(1): 444–457.
30. Lindorff-Larsen K, Piana S, Palmo K, Maragakis P, Klepeis JL, Dror RO, Shaw DE. Improved side-chain torsion potentials for the Amber ff99SB protein force field. *Proteins*. 2010; 78(8):1950–1958. [PubMed: 20408171]
31. Mark P, Nilsson L. Structure and Dynamics of the TIP3P, SPC, and SPC/E Water Models at 298 K. *J Phys Chem A*. 2001; 105(43):9954–9960.
32. Darden T, York D, Pedersen L. Particle mesh Ewald: An  $N \cdot \log(N)$  method for Ewald sums in large systems. *J Chem Phys*. 1993; 98(12):10089–10092.
33. Pierce B, Hourai Y, Weng Z. Accelerating protein docking in ZDOCK using an advanced 3D convolution library. *PLoS One*. 2011
34. Morris G, Goodsell D, Halliday R, Huey R, Hart W, Belew R, Olson A. Automated docking using a Lamarckian genetic algorithm and an empirical binding free energy function. *J Comput Chem*. 1998; 19(14):1639–1662.
35. Konc J, Konc JT, Penca M, Janežič D. Binding-sites Prediction Assisting Protein-protein Docking. *Acta Chim Slov*. 2011; 58(3):396–401. [PubMed: 24062097]
36. Liwo A, Kaźmierkiewicz R, Czaplewski C, Groth M, Oldziej S, Wawak R, Rackovsky S, Pincus M, Scheraga H. United-residue force field for off lattice protein structure simulations: III. Origin of backbone hydrogen bonding cooperativity in united-residue potentials. *J Comput Chem*. 1998; 19:259–276.
37. Liwo A, Czaplewski C, Oldziej S, Rojas AV, Kaźmierkiewicz R, Makowski M, Murarka R, Scheraga H. Simulation of protein structure and dynamics with the coarse-grained UNRES force field. *Coarse-Graining of Condensed Phase and Biomolecular Systems Coarse-Graining Condensed Phase Biomol Syst*. 2008; (8):107–122.

38. Liwo A, Czaplewski C, Pillardy J, Scheraga H. Cumulant-based expressions for the multibody terms for the correlation between local and electrostatic interactions in the united-residue force field. *J Chem Phys.* 2001; 115:2323–2347.
39. Murtagh F. Multidimensional clustering algorithms. *Compstat Lect Vienna Phys Verlag.* 1985 1985.
40. Murtagh, F.; Heck, A. Kluwer Academic Publishers. Kluwer Academic Publishers; 1998. Multivariate data analysis.
41. Ward JH. Hierarchical groupings to optimize an objective function. *J Amer Stat Assoc.* 1963; 58:234–244.
42. Vreven T, Hwang H, Weng Z. Integrating atom-based and residue-based scoring functions for protein-protein docking. *Protein Sci.* 2011; 20(9):1576–1586. [PubMed: 21739500]
43. Steczkiewicz K, Zimmermann MT, Kurcinski M, Lewis BA, Dobbs D, Kloczkowski A, Jernigan RL, Kolinski A, Ginalski K. Human telomerase model shows the role of the TEN domain in advancing the double helix for the next polymerization step. *Proc Natl Acad Sci U S A.* 2011; 108(23):9443–9448. [PubMed: 21606328]
44. Rojas AV, Liwo A, Scheraga HA. Molecular dynamics with the United-residue force field: ab initio folding simulations of multichain proteins. *J Phys Chem B.* 2007; 111(1):293–309. [PubMed: 17201452]
45. Shi R, Proteau A, Villarroya M, Moukadiri I, Zhang L, Trempe JF, Matte A, Armengod ME, Cygler M. Structural basis for Fe-S cluster assembly and tRNA thiolation mediated by IscS protein-protein interactions. *PLoS Biol.* 2010; 8(4):e1000354. [PubMed: 20404999]
46. Roy A, Kucukural A, Zhang Y. I-TASSER: a unified platform for automated protein structure and function prediction. *Nat Protoc.* 2010; 5(4):725–738. [PubMed: 20360767]
47. Roy A, Yang J, Zhang Y. COFACTOR: an accurate comparative algorithm for structure-based protein function annotation. *Nucleic Acids Res.* 2012; 40:W471–W477. [PubMed: 22570420]
48. Zhang Y, Skolnick J. TM-align: a protein structure alignment algorithm based on the TM-score. *Nucleic Acids Res.* 2005; 33:2302–2309. [PubMed: 15849316]
49. Krieger E, Joo K, Lee J, Raman S, Thompson J, Tyka M, Baker D, Karplus K. Improving physical realism, stereochemistry, and side-chain accuracy in homology modeling: Four approaches that performed well in CASP8. *Proteins Struct Funct Bioinforma.* 2009; 77:114–122.

## Abbreviations

<b>Hsp70</b>	70 kilodalton heat shock proteins
<b>Yfh1</b>	Yeast Frataxin Homolog
<b>Nfs1</b>	Cysteine desulfurase, mitochondrial
<b>Isd11</b>	Iron-sulfur protein biogenesis, desulfurase-interacting protein 11
<b>UNRES</b>	UNited RESidue force field
<b>Fe-S</b>	Iron-sulfur cluster
<b>kDa</b>	kilo dalton
<b>ATP</b>	Adenosine triphosphate
<b>I-TASSER</b>	Iterative Threading ASSEmbly Refinement
<b>YASARA</b>	Yet Another Scientific Artificial Reality Application
<b>ISC</b>	iron-sulphur cluster



**Figure 1.**

The UNRES model of polypeptide chains. The interaction sites are peptide-group (p) and side-chain centers (SC) attached to the corresponding  $C^\alpha$  atoms with different  $C^\alpha \dots SC$  bond lengths,  $d_{SC}$ . The peptide groups are represented as gray circles, and the side chains are represented as gray ellipsoids of different sizes for appropriate residues. The  $\alpha$ -carbon atoms are represented by small white circles. The geometry of the chain can be described either by the virtual-bond vectors  $dC_i$  (from  $C_i^\alpha$  to  $C_{i+1}^\alpha$ ),  $i = 1, 2, \dots, n - 1$ , and  $dX_i$  (from  $C_i^\alpha$  to  $SC_i$ ),  $i = 2, \dots, n - 1$ , represented by thick lines, where  $n$  is the number of residues, or in terms of virtual-bond lengths, backbone virtual-bond angles  $\theta_i$ ,  $i = 1, 2, \dots, n - 2$ , backbone virtual-bond-dihedral angles  $\gamma_i$ ,  $i = 1, 2, \dots, n - 3$ , and the angles  $\alpha_i$  and  $\beta_i$ ,  $i = 2, 3, \dots, n - 1$ , that describe the location of a side chain with respect to the coordinate frame defined by  $C_{i-1}^\alpha$ ,  $C_i^\alpha$ , and  $C_{i+1}^\alpha$ .

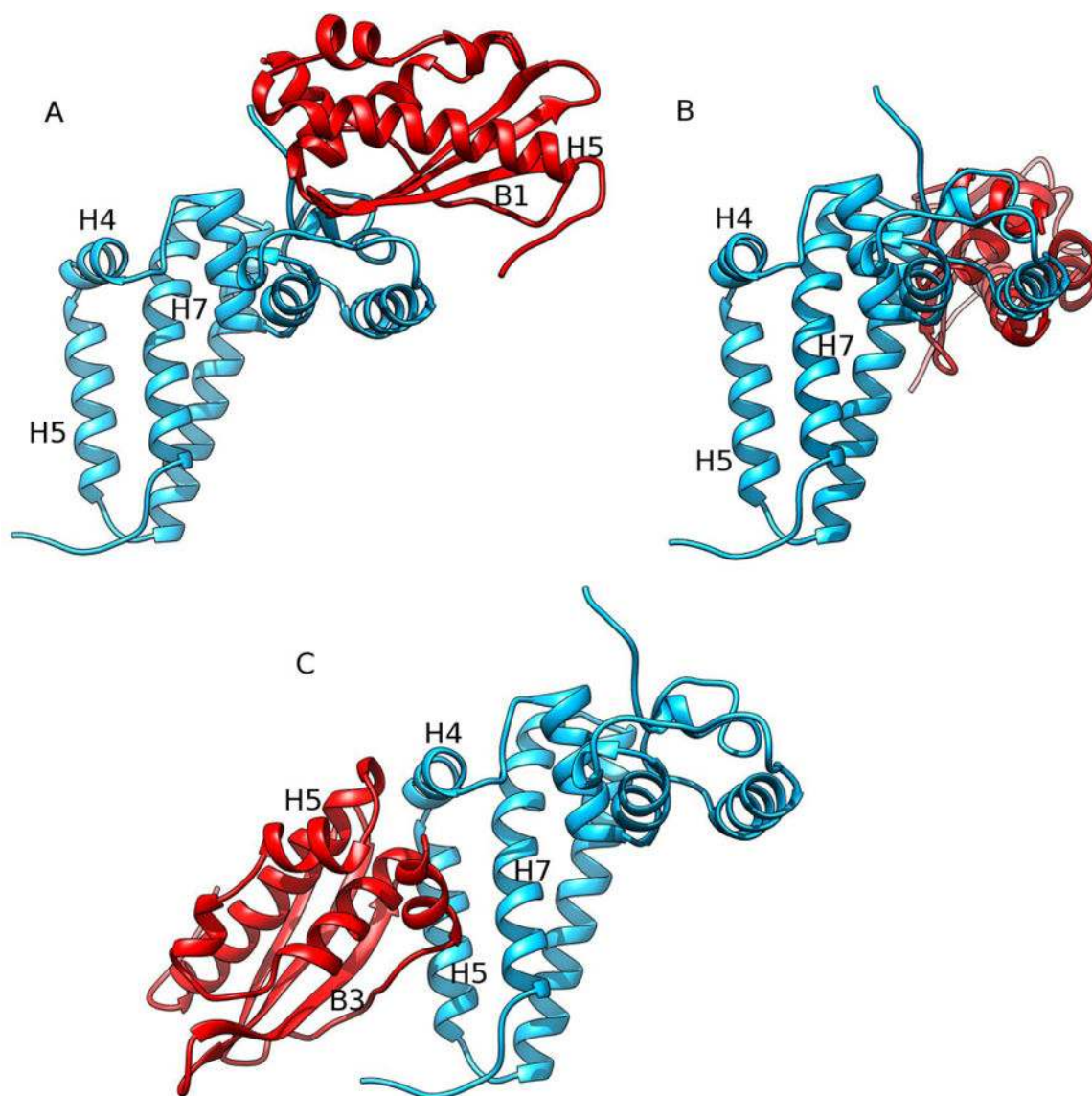


**Figure 2.**  
Three main positions of Isu1 (red) with respect to Jac1 (blue) from global docking with the ZDOCK server for the Isu1-Jac1 complex.

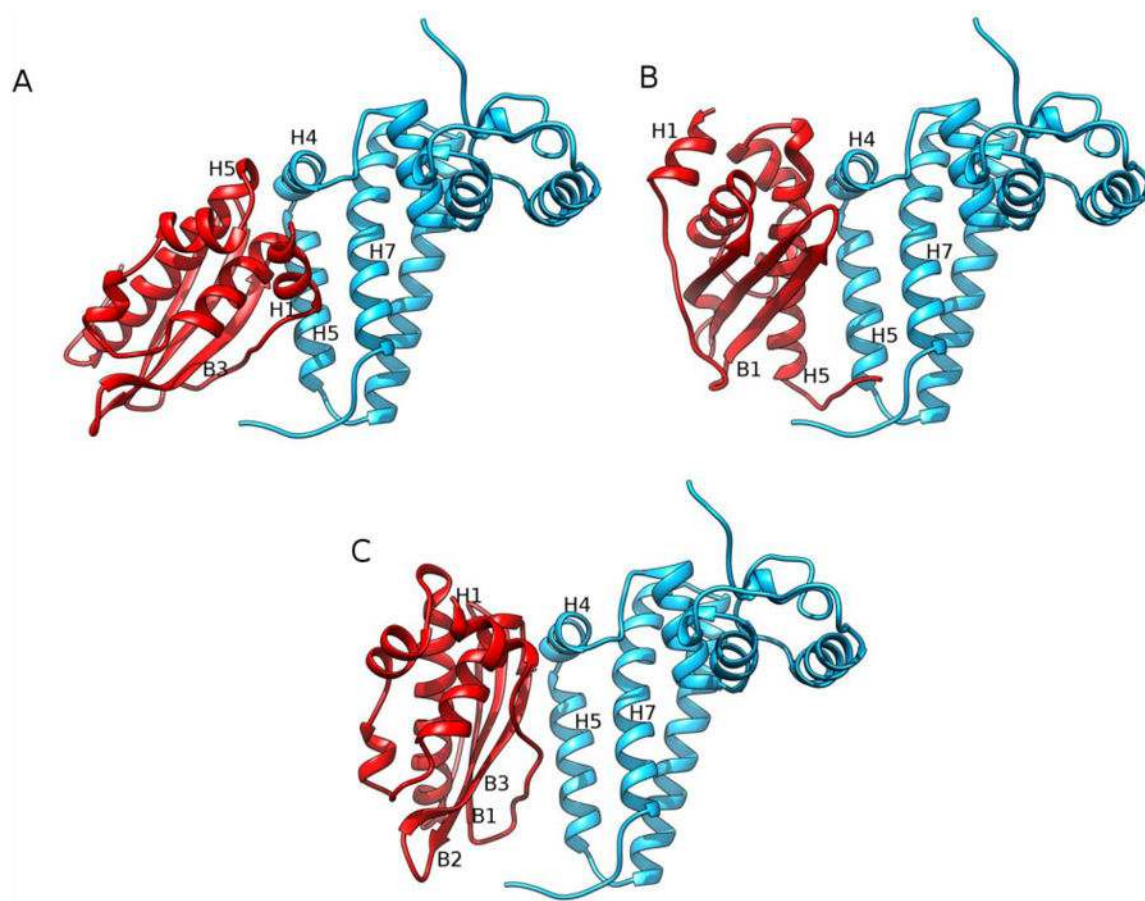


**Figure 3.**  
Results for local docking of Isu1 (red) to Jac1 (blue); A) Model 1; B) Model 2; C) Model 3.

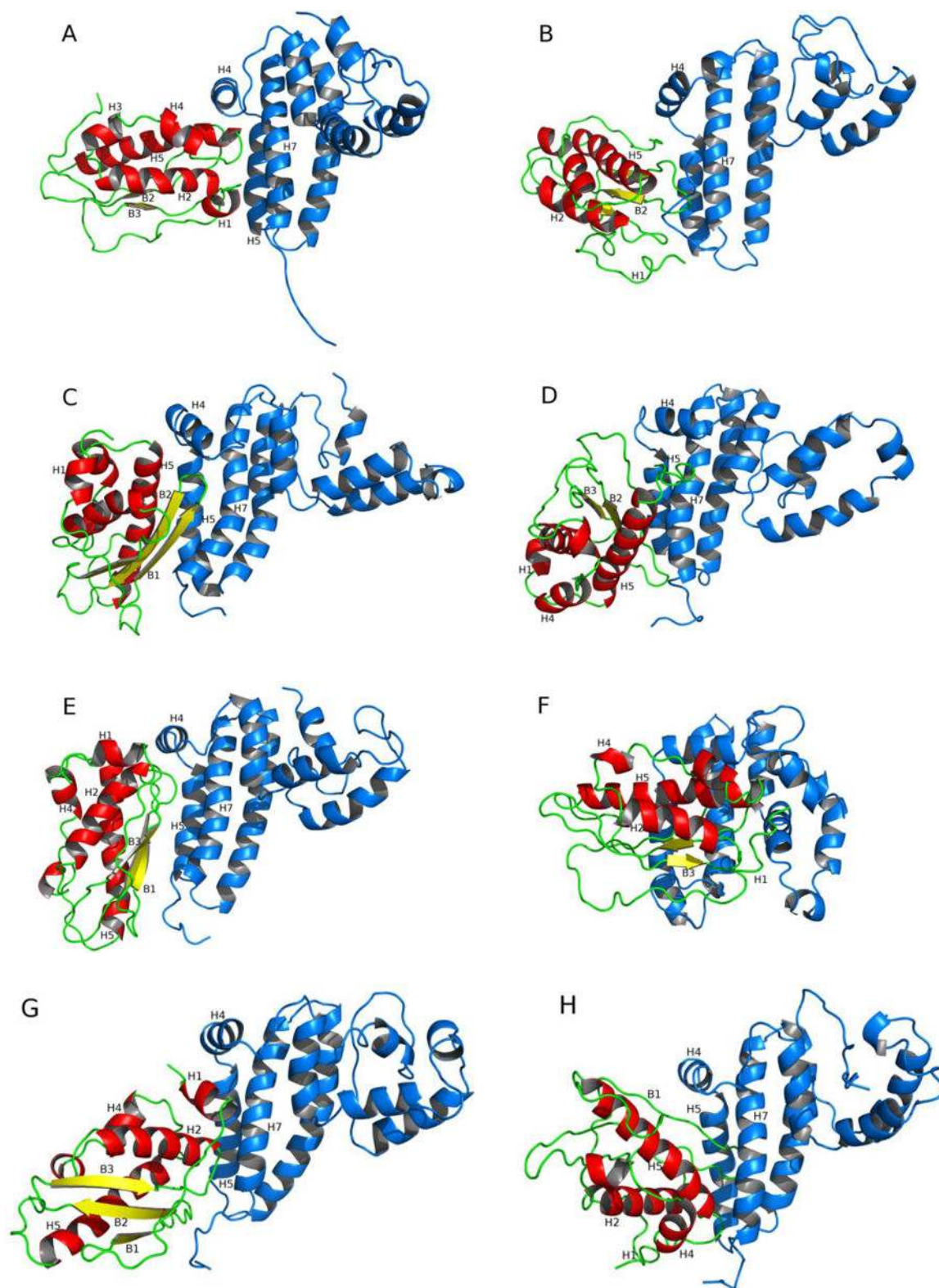


**Figure 4.**

Representative structures of each of groups A to G of the Isu1/Jac1 complex. Jac1 is represented as a blue surface. Isu1 is shown as helices colored red and  $\beta$ -strands colored yellow.

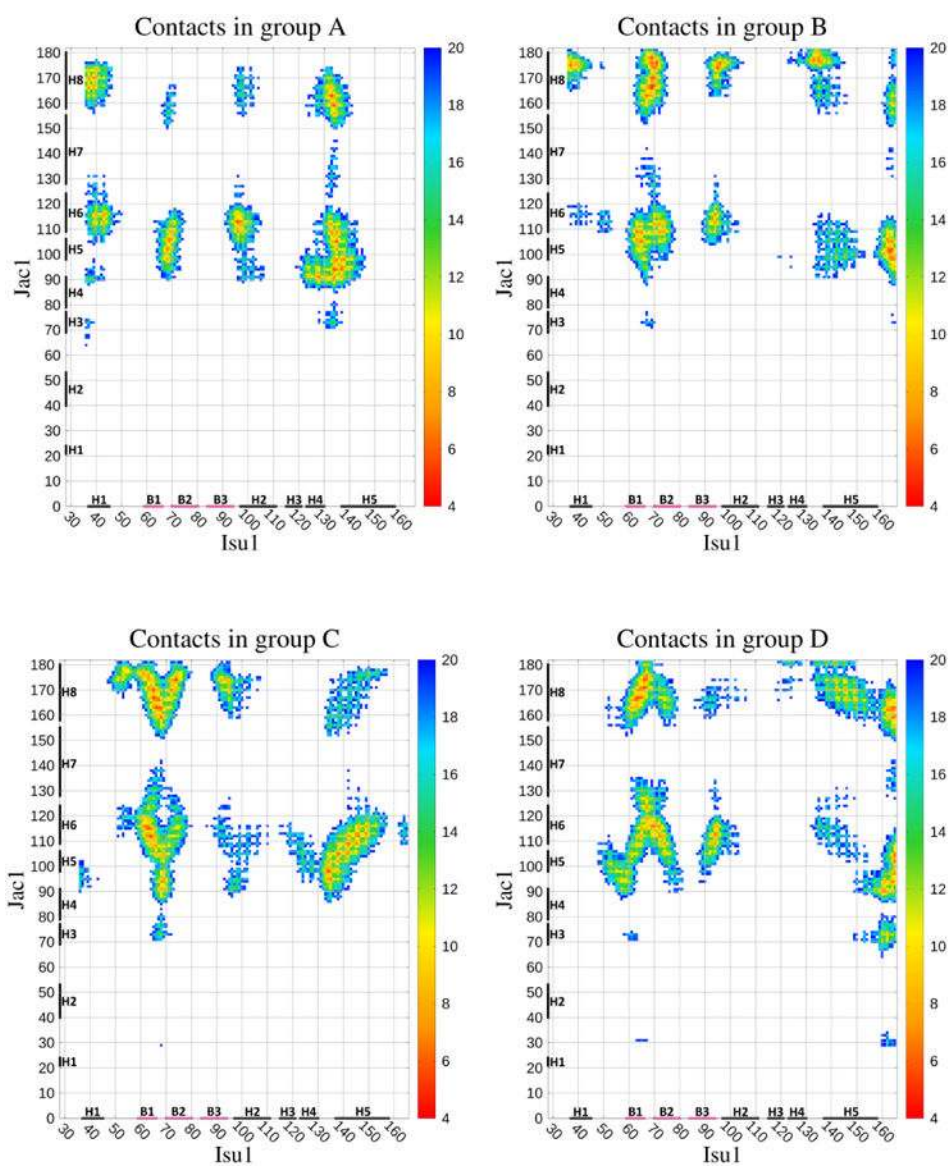
Author Manuscript

Author Manuscript

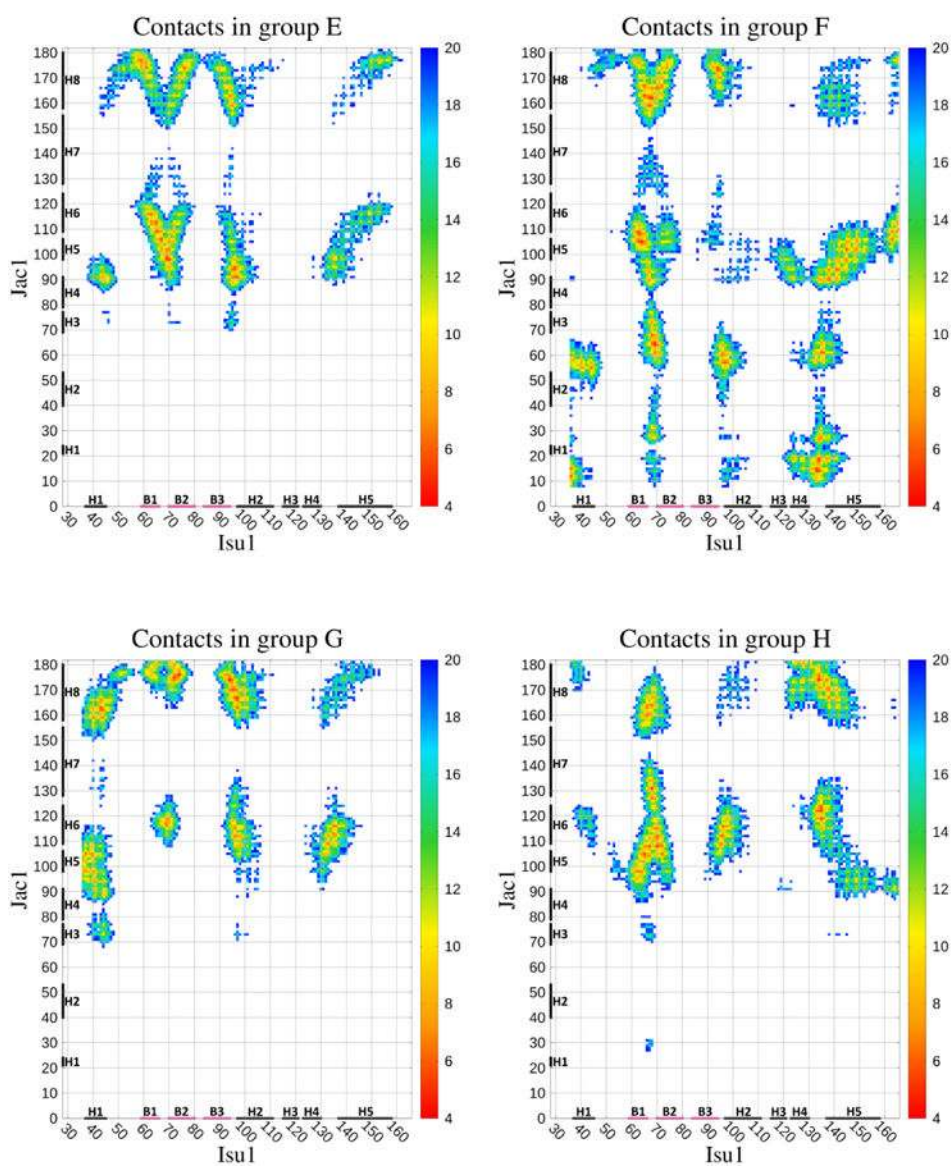
Author Manuscript

Author Manuscript









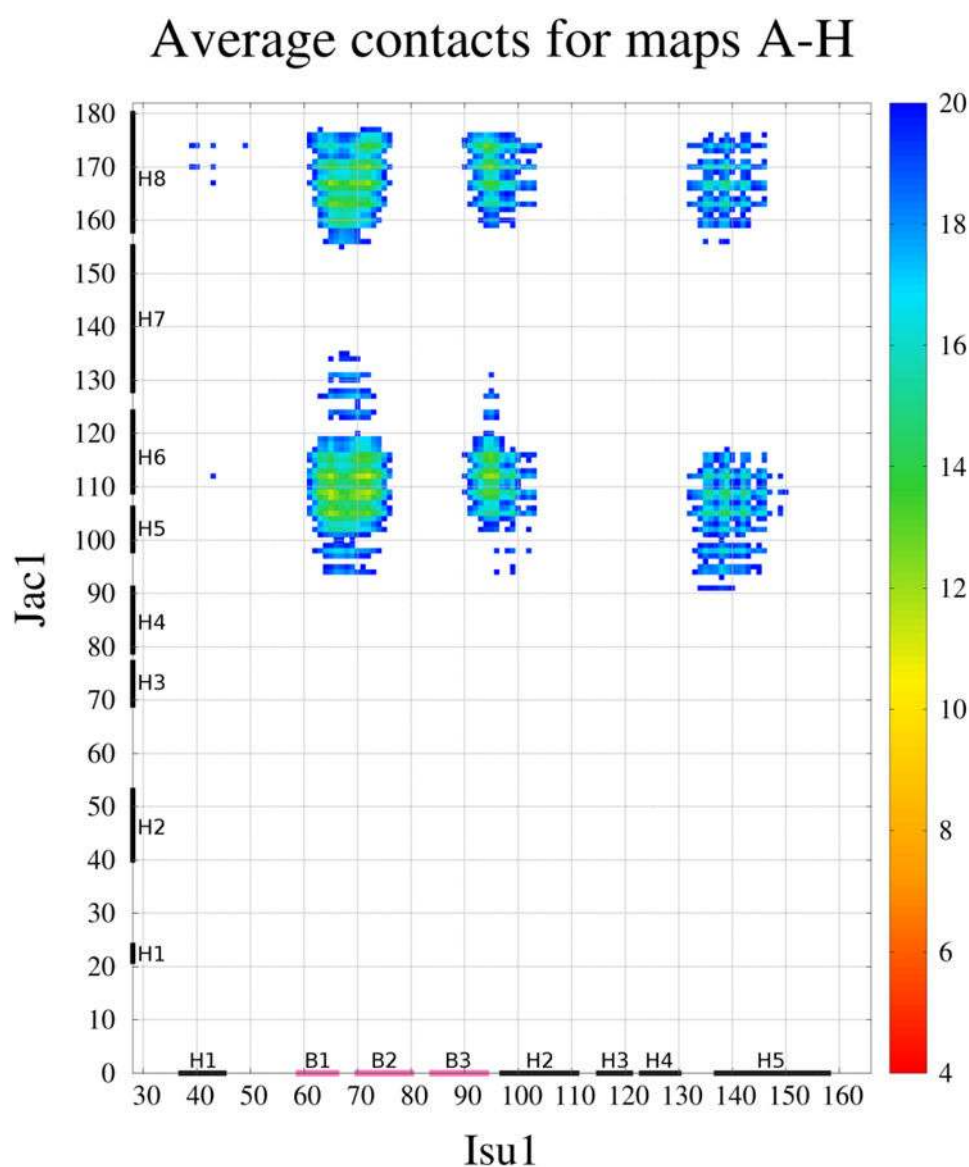


**Figure 5.**

Distance maps ( $C^{\alpha} \dots C^{\alpha}$  atom distances smaller than 20 Å) of representative structures of each group of the Isu1/Jac1 complex. The  $C^{\alpha} \dots C^{\alpha}$  atom distances are shown in color scale in Å from red (smallest distances to dark blue (20 Å)). Distances greater than 20 Å are not mapped. Close contacts occur when residues are at a distance shorter than 7 Å. Secondary structure elements are marked by lines at the bottom with labels of the respective helix (H, black) or β-strand (B, pink) on the x and y axes. Residue numbers are marked on the horizontal axis and on the vertical axis.

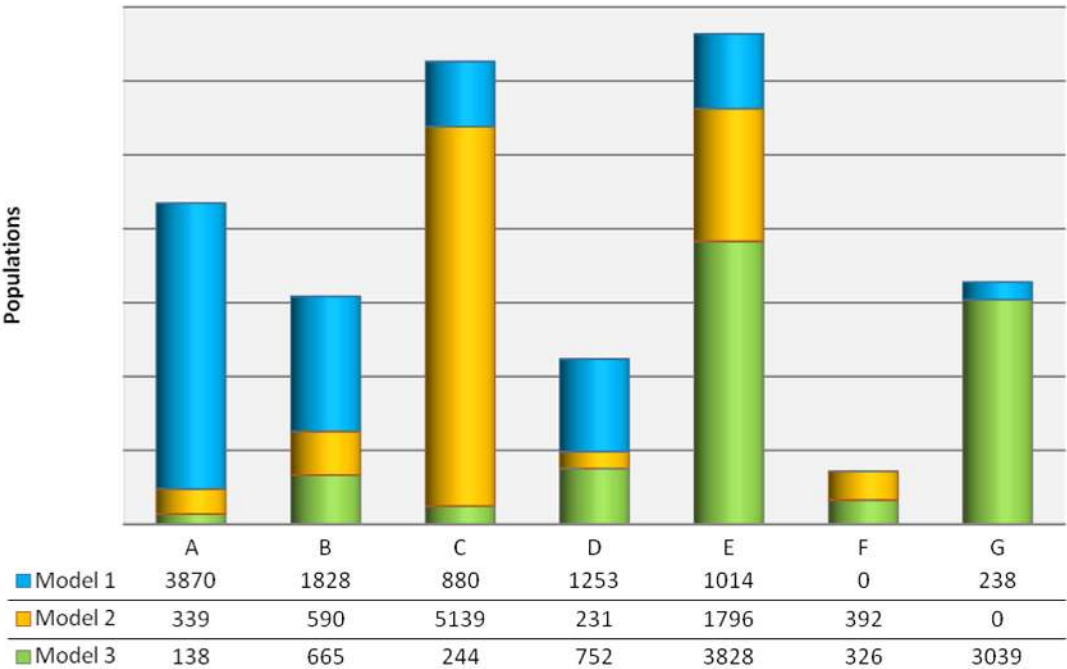


**Figure 6.**  
Cumulative populations of all groups of conformations in all UNRES/MD simulations started from Model 1, Model 2, and Model 3, respectively.

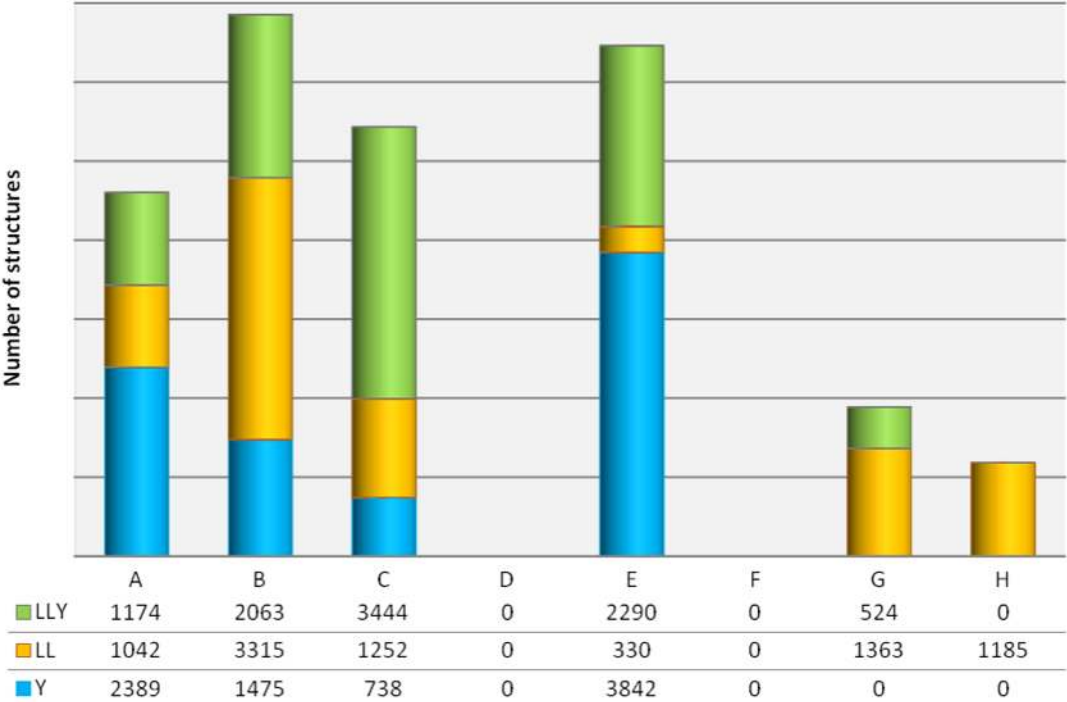


**Figure 7.**  
Cumulative populations of all groups of conformations in all UNRES/MD simulations of all Isu1-Jac1 complexes with mutated Isu1.

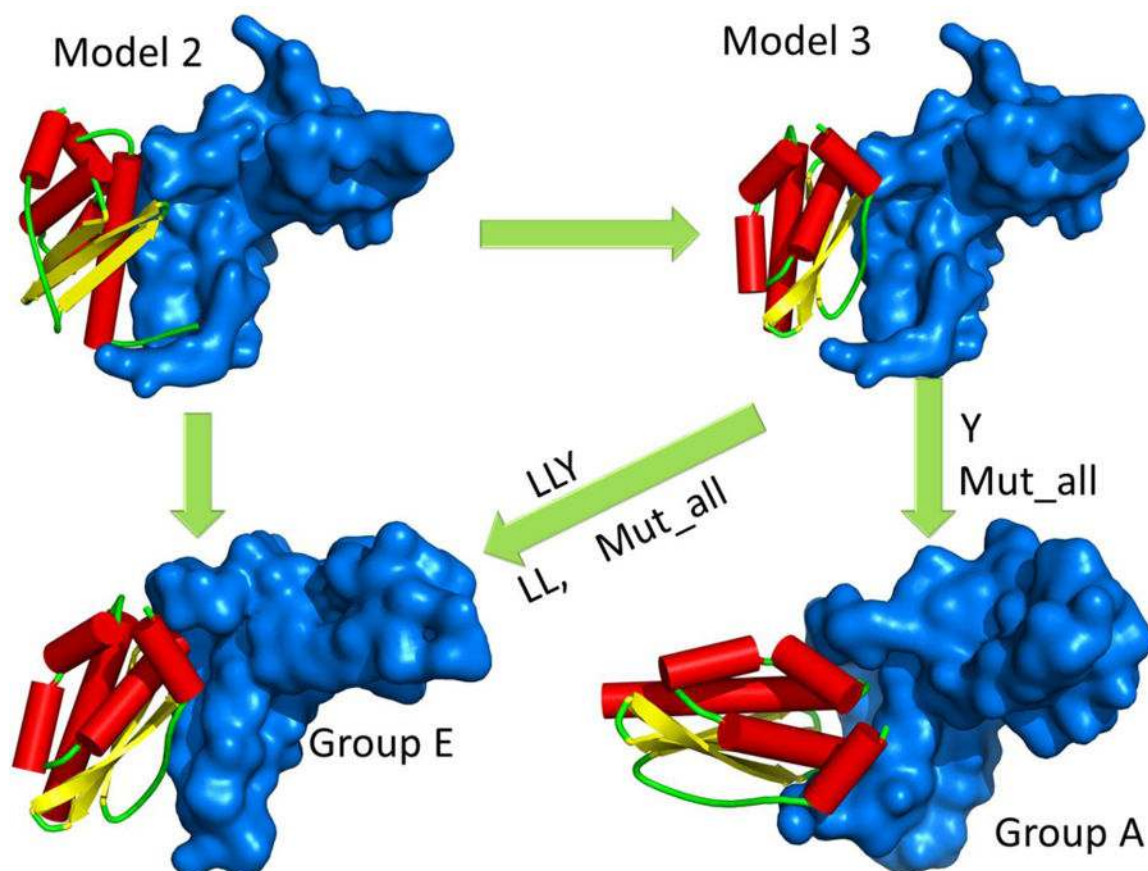


**Figure 8.**

A scheme to illustrate the structural changes caused by particular mutations. The Jac1 protein is marked as a blue surface. Isu1 is in a cartoon representation, in which helices are colored red and  $\beta$ -sheets are colored yellow. As illustrated, Model 2 during simulation, Model 2 goes to Model 3 and to Group E. After mutations, Model 3 goes to group E and group A.

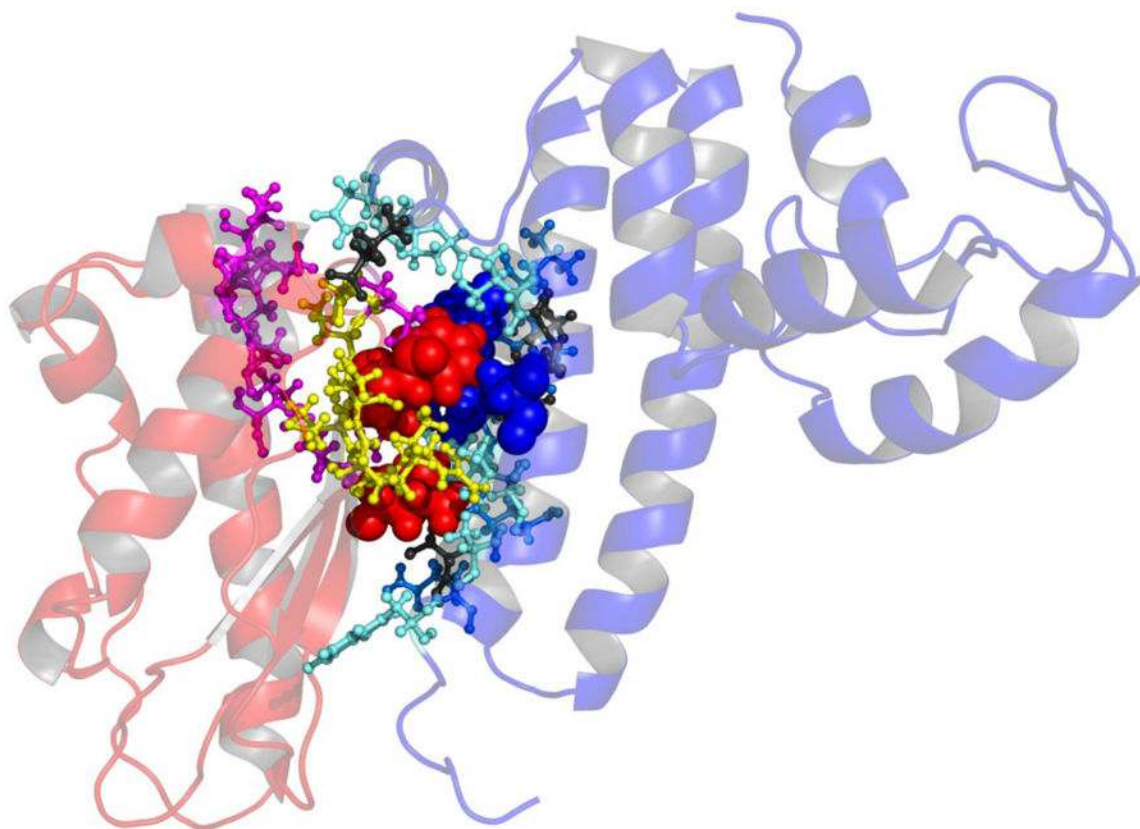


**Figure 9.**

A representative structure of the Isu1-Jac1 complex (from group C) obtained by molecular docking followed by UNRES/MD simulations. The bulk of the structure is shown in cartoon representation (blue: Jac1, red: Isu1), while the residues of the binding interface shown in atomic-detailed representation. The Jac1 residues found important for binding both in this work and in earlier experimental studies (L<sub>105</sub>, L<sub>109</sub>, and Y<sub>163</sub>)<sup>3</sup> are colored dark-blue and shown in space-filling representation; the Jac1 residues found important for binding in this study and suggested by experiment to be important in binding (L<sub>104</sub>, K<sub>107</sub>, D<sub>110</sub>, D<sub>113</sub>, E<sub>114</sub>, and Q<sub>117</sub>) are colored blue and shown in ball-and-stick representation, residues that are found important for binding are colored cyan and shown in ball-and stick representation (residues N<sub>95</sub>, T<sub>98</sub>, P<sub>102</sub>, H<sub>112</sub>, V<sub>159</sub>, L<sub>167</sub>, A<sub>170</sub>, W<sub>174</sub>)<sup>1</sup>, while the residues of Jac1 found by simulations to make less tight contacts with Isu1 but also possibly important for binding (residues E<sub>91</sub>, V<sub>108</sub>, S<sub>116</sub>, and E<sub>160</sub>) are colored dark-gray and shown in ball-and-stick representation. The same hierarchy of representation and colors red (L<sub>63</sub>, V<sub>72</sub>, and F<sub>94</sub>), yellow (V<sub>64</sub>, A<sub>66</sub>, D<sub>71</sub>, M<sub>73</sub>, R<sub>74</sub>, K<sub>92</sub>, T<sub>93</sub>, C<sub>96</sub>), and magenta (G<sub>65</sub>, G<sub>70</sub>, G<sub>95</sub>, V<sub>135</sub>, K<sub>136</sub>, H<sub>138</sub>, C<sub>139</sub>, L<sub>142</sub>) are used for the residues of Isu1 found to be important for binding by both simulation and experiment, by simulation and, to a lesser extent, by experiment, and by simulation only, respectively.



**Table 1**C-score values of the models from I-TASSER and YASARA.<sup>25, 46, 47</sup>

Name	C-score <sup>a</sup>	Exp. TM-Score <sup>b</sup>	Exp. RMSD	No. of decoys <sup>c</sup>	Cluster density <sup>d</sup>
Model 1	0.63	0.80 ± 0.09	3.2 ± 2.3	8308	0.4356
Model 2	-1.25	-	-	1263	0.0662
Model 3	-1.20	-	-	2327	0.0696
Model 4	0.04	-	-	4573	0.2398
YASARA model 1	-0.506 <sup>e</sup>	-	-	-	-
YASARA model 2	-0.511 <sup>e</sup>	-	-	-	-
YASARA model 3	-1.067 <sup>e</sup>	-	-	-	-
YASARA model 4	-1.088 <sup>e</sup>	-	-	-	-
YASARA hybrid	-0.193 <sup>e</sup>	-	-	-	-

<sup>a</sup>C-score<sup>25</sup> is a confidence score for estimating the quality of the predicted models.<sup>b</sup>TM-score<sup>48</sup> is a standard method for measuring structural similarity between two molecules.<sup>c</sup>Number of replicas (structures) in each model.<sup>d</sup>The cluster density (original term from ref. 46) or cluster population is defined as the number of structures present in a given cluster. Higher cluster density means that the structure appears more often in the simulation trajectory and has a better quality model.<sup>e</sup>in YASARA<sup>49</sup>, the overall quality of a model is given by the Z-score value, which is a weighted average of the individual Z-scores corresponding to quality of dihedral angles and packing.

**Table 2**

RMSD values of structures of Isu1 and Jac1 in complexes of groups A-H from the initial structures of isolated components.

Group	RMSD[Å] of a structures			
	Isu1	Jac1 domains <sup>a</sup>		
		N-terminal	C-terminal	Whole
<b>A</b>	4.289	5.523	5.193	6.058
<b>B</b>	5.292	3.914	6.582	6.202
<b>C</b>	4.530	4.674	5.117	6.110
<b>D</b>	3.617	4.297	4.725	7.947
<b>E</b>	4.998	5.450	4.062	6.431
<b>F</b>	3.497	8.182	4.507	9.829
<b>G</b>	4.466	5.497	4.065	6.382
<b>H</b>	4.762	6.689	5.054	7.537

<sup>a</sup>N-terminal domain – residues 11-84; C-terminal domain – residues 101-181; whole structure – residues 8-181 of Jac1.